



CHEMICAL SCIENCES

Theoretical study of Gibbs free energy and NMR chemical shifts, of the effect of methyl substituents on the isomers of (E)-1-(α,β -Dimethylbenzyliden)-2,2-diphenylhydrazine.

JUAN CARLOS RAMÍREZ-GARCÍA, RICARDO VÁZQUEZ-RAMÍREZ, MARÍA EUGENIA PATIÑO, CARLA AGUIRRE-CABRERA, VLADIMIR CARRANZA & CARMEN MÁRIA GONZÁLEZ ÁLVAREZ

Abstract: A theoretical analysis of free Gibbs Energy and NMR ^1H ^{13}C chemical shifts of the effect of introduce methyl groups on diphenyl rings, to produce different isomers of (E)-1-(α,β -dimethylbenzylidene)-2,2-diphenylhydrazine, is presented. IR vibrational frequencies, Mulliken charges, molecular electrostatic potential (MEP), Gibbs free energy (G) and ^1H - and ^{13}C -NMR chemical shifts were obtained by theoretical calculations. In this analysis it was found that the position of the methyl group affects the values of the ^1H - and ^{13}C -NMR chemical shifts and the ΔG and ΔH thermodynamic properties of formation and reaction, these properties vary with the same trend, for the isomers studied. Gibbs free energy calculations show that the theoretical (E)-1-(3,4-Dimethylbenzylidene)-2,2-diphenylhydrazine isomer is the most stable, which explains the success of the experimental synthesis of this compound among the other isomers. For this molecule, the C of the HC=N group is the most nucleophilic and the H is the least acidic. The ^1H -NMR chemical shifts of protons show a strong correlation with the C=N distance. It was also observed that methyl affects the $\nu(\text{C}=\text{N})$ frequencies, the C=N distance increases when the inductive effect of the methyl groups is in the structure.

Key words: Gibbs Energy, Enthalpy, NMR, DFT, Hydrazines, Theoretical calculations.

INTRODUCTION

Hydrazones are a class of organic compounds with the C=N-N structure. This functional group has been extensively studied and used in supramolecular chemistry on self-assembled systems, organic synthesis and medicinal chemistry, among other (Su & Aprahamian 2014). These compounds exhibit diverse biological and pharmacological properties, some of the reported properties are antimicrobial, anti-inflammatory, analgesic, antifungal, antituberculosis, antiviral, anticancer, antiplatelet, antimalarial, anticonvulsant, cardioprotective, anthelmintic,

antiprotozoal, ant trypanosome, and ant schistosomiasis (Verma et al. 2014, Zaidi et al. 2018). The multiple applications of hydrazones are due to their stability against hydrolysis, as well as the diversity of reactions that the C=N-N group can undergo (Verma et al. 2014) because the hydrazone structure has a nucleophilic character (Nigst et al. 2012) with its two of N classes (imine and amine) that allows its use in various fields; it also has an imine carbon that is both electrophilic and nucleophilic in character; and a configurational isomerism derived from the intrinsic nature of the CN double bond; and in most cases, an acidic

N-H proton. These particular features give the hydrazone group its physical and chemical properties, as well as playing a crucial role in determining the sort of hydrazones applications, vibrational frequencies, NMR chemical shifts, and thermodynamic functions of isomers formation. DFT methods have been used to predict thermochemical properties, the B3LYP/6-311++G(d,p) method/basis set is a combination of a hybrid DFT approach and a Gaussian-type orbital triple basis set (Lee & Sosa 1994) which incorporates diffuse and polarization functions approach is a good compromise between quality of calculated data and computational speed-up (Becke 1993). Density functional (DFT) methods are a good alternative to high-cost calculations (Hamzehloueian 2017) describes frequencies better they can also show charge transference in molecules with similar electronic properties (Balakit et al. 2020) and predict in good agreement with experimental values which have been used to predict thermochemical properties as reported (Curtiss et al. 1997) report. Employing vibrational frequency analysis, zero-point energy (ZPE) and thermal correction were used to obtain thermodynamic data, such as standard enthalpy, entropy and Gibbs free energy reaction and formation changes (Bauerfeldt et al. 2005, Sousa et al. 2013). Thermochemical calculations of different compounds have been reported, where they used the B3LYP method to obtain theoretical enthalpies of substituted hydrazine molecules (Wilcox et al. 2002, Wilcox & Bauer 2003, Bohn & Klapotke 2004). Some reports compare data of vibrational frequencies, ^1H and ^{13}C NMR chemical shifts, UV-Vis. spectra with thermodynamic data of molecules related to hydrazone derivatives for different purposes, as in (Tanak & Toy 2016) which compared experimentally and theoretical data from a Schiff basis to identifying the most stable conformer for the anticonvulsant agent

(Haress et al. 2016) in (Arshad 2015) chemical reactivity indices predict the highest and lowest activity for four triazine-based hydrazone derivatives, with the help of the molecular electrostatic potential (MEP) predicting the most reactive site for electrophilic attack (Shin & Jung 2022). Has been reported theoretical calculations (Benassi et al. 2008) analyzing the conformational equilibria, finding the most stable equilibrium structure and explain binding characteristics. These thermodynamic data were calculated with vibrational analysis and ^1H and ^{13}C NMR chemical shifts in different solvents, shows a good correlation with experimental data. Some reports show a trend between NMR signals with thermodynamic properties of some conformational isomers, and distinguish differences between reactants and products (Eliel 1960, Juaristi & Muñoz-Muñiz 2001, Eliel & Martin 1968, Souza et al. 2018, Krishnan 2019). There are some reports which relate thermodynamic properties with NMR signals of core magnetization to the Gibbs free energy obtained by frequency analysis with electronic energies, zero-point energy and thermal effects (Landerville et al. 2010, Ruzsinszky et al. 2003). These are based on the assumption that the conformational equilibrium ($A \leftrightarrow B$) is reached rapidly on the NMR time-scale, the chemical shift for a given nucleus is a mol fraction-weighted average over all the chemical species where the nucleus is present. Using conformational equilibria $K_{eq} = (\delta_a - \delta) / (\delta - \delta_e)$, where δ is the chemical shift, to obtain free energy differences with $\Delta G^0 = -RT \ln K_{eq}$, where ΔG^0 is the standard Gibbs free energy. According to statistical mechanics the Gibbs free energies depend on degrees of freedom: translational, electronic, rotational, and vibrational which are included in the partition function (Atkins et al. 2018). The importance of the partition function is because contains all the information needed

to obtain thermodynamic properties of chemical species, just like the wave function in quantum mechanics. The total partition function is the product of the partition functions of individual modes. The contribution of nuclear energy to the total energy is negligible, but the total partition function raises information of the nuclear contribution. NMR spectroscopy relies on the fact that the states are not exactly equally populated, but in the context of statistical thermodynamics the contribution to the internal energy and population differences are negligible (Jeschke 2015, Hanson et al. 2016). The frequencies calculated with B3LYP/6-311++G(d,p) are used to calculate the zero-point energies and other thermal corrections to the total energy; in the calculations the zero-point energy, is the zero energy at absolute zero to fit the Gibbs Free Energy, entropy and enthalpy (Frisch et al. 1996). Previous reports have experimentally obtained A20 and A215 among other possible isomers, it will be interesting to know why was obtained only A215 isomer and why not others. In this report, calculations of ^1H and ^{13}C NMR chemical shifts, standard enthalpy, entropy and Gibbs free energy of reaction and formation, at zero point energy (ZPE) (Ruzsinszky et al. 2003) calculation with thermal correction are presented. With the aim of finding why some isomers is obtained and no others, besides to find a relationship between the location of the substituents in the hydrazone isomers of the (E)-1-(α,β -Dimethylbenzylidene)-2,2-diphenylhydrazines, with the thermodynamic state functions and the chemical shifts.

MATERIALS AND METHODS

Molecules studied

Theoretical models of these molecules were calculated (E)-1-Benzylidene-2,2-diphenylhydrazine (A20),

(E)-1-(2,3-Dimethylbenzylidene)-2,2-diphenylhydrazine (A211), (E)-1-(2,4-Dimethylbenzylidene)-2,2-diphenylhydrazine (A212), (E)-1-(2,5-Dimethylbenzylidene)-2,2-diphenylhydrazine (A213), (E)-1-(2,6-Dimethylbenzylidene)-2,2-diphenylhydrazine (A214), (E)-1-(3,4-Dimethylbenzylidene)-2,2-diphenylhydrazine (A215), (E)-1-(3,5-Dimethylbenzylidene)-2,2-diphenylhydrazine (A216) the structures are shown in Figure 1. Molecules A20 and A215 were obtained experimentally (Mendoza et al. 2012, 2011).

Theoretical calculations

Molecular geometries of molecules of Figure 1 were optimized with B3LYP/6-311++G(d,p) theory (Becke 1993) with Gaussian 09 (Frisch et al. 2016). Vibrational frequencies were calculated in the ground state, the positive values of all calculated vibrational frequencies indicate that the optimized molecular structure is stable, the frequencies computed include well-known systematic errors (Merrick et al. 2007, Scott & Radom 1996, Andersson & Uvdal 2005). Enthalpies of reaction and formation were calculated using the sum of electronic and thermal enthalpies from Gaussian output for the products and reactants, Gibbs free energy is calculated adding the entropy term (Ochterski et al. 1995). Thermodynamic properties were calculated using Zero-point energies and thermal corrections were calculated at 298.15K based on unscaled frequencies (Ruzsinszky et al. 2003). For ^1H and ^{13}C NMR, molecular geometry of molecules of figure 1, were optimized at B3LYP/6-311++G(d,p) level in $(\text{CD}_3)_2\text{CO}$ solvent ($\epsilon = 20.7$) by IEFPCM (integral equation formalism polarizable continuum model) (Nguyen 2021). Chemical shifts were calculated using the Gauge-Invariant Atomic Orbital (GIAO) method (Wolinski et al. 1990) using B3LYP/6-311++G(d,p), over the most stable conformers, similar studies

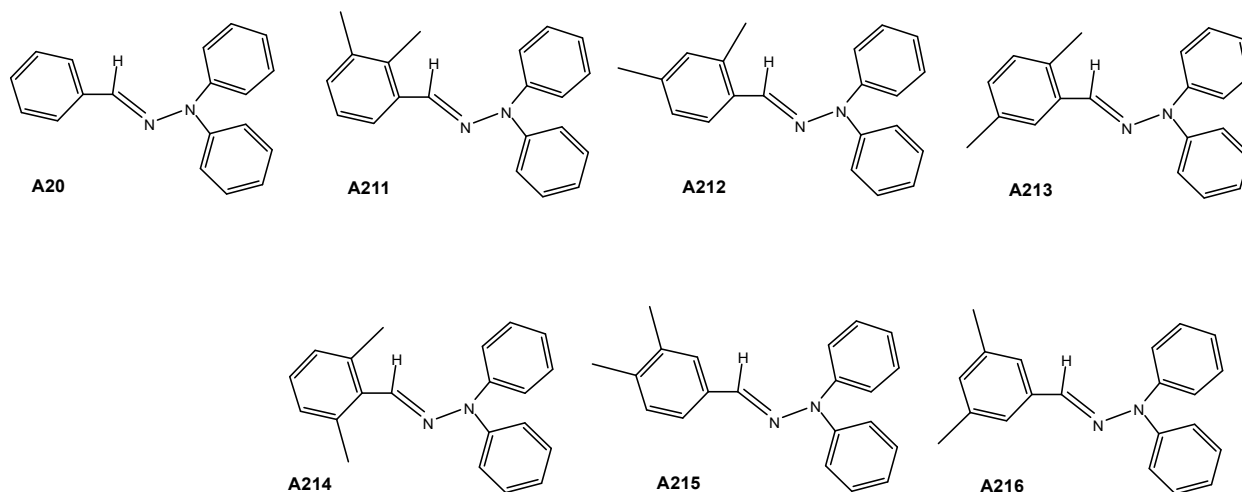


Figure 1. Molecules modeled for theoretical calculations (*E*)-1-Benzylidene-2,2-diphenylhydrazine (**A20**), (*E*)-1-(2,3-Dimethylbenzylidene)-2,2-diphenylhydrazine (**A211**), (*E*)-1-(2,4-Dimethylbenzylidene)-2,2-diphenylhydrazine (**A212**), (*E*)-1-(2,5-Dimethylbenzylidene)-2,2-diphenylhydrazine (**A213**), (*E*)-1-(2,6-Dimethylbenzylidene)-2,2-diphenylhydrazine (**A214**), (*E*)-1-(3,4-Dimethylbenzylidene)-2,2-diphenylhydrazine (**A215**), (*E*)-1-(3,5-Dimethylbenzylidene)-2,2-diphenylhydrazine (**A216**).

have been reported (Dege et al. 2022, Gökce et al. 2022). For UV-Vis. computations, the electronic absorption maximum wavelengths (K_{max}) were computed using the time-dependent DFT (TD-DFT) method using B3LYP/6-311++G(d,p) theory (Cancés et al. 1997, Jacquemin et al. 2008). The molecular electrostatic potential (MEP) (Murray & Politzer 2011) for each isomer was calculated using the optimized molecular geometries obtained with B3LYP/6-311++G(d,p). To find any change of the MEP with the changes of methyl position in one of the phenylhydrazine rings in the different isomers (Shin & Jung 2022). Molecular Electrostatic Potential was calculated and visualized with Spartan¹⁴ suite of programs (Wavefunction 2014).

RESULTS AND DISCUSSION

Table I shows the calculated thermochemical data calculated for the molecules, Table II shows the ^1H and ^{13}C NMR chemical shifts for various atoms of the molecule in Figure 2. Table III shows the characteristic IR and UV ν_{max} vibrational frequencies. Table IV shows

the geometrical distances for the hydrazine atoms. Figures 3, 4 and 5 show the behavior of the thermodynamic data and ^{13}C and ^1H NMR chemical shifts from Tables I and II. They were modeled and optimized using. In table I the theoretical values of thermodynamic quantities of reaction and formation: standard enthalpy and Gibbs free energy and total energies of the isomers modeled in Figure 1.

Thermodynamic Quantities of Reaction and Formation

The thermochemical values $\Delta_r H$ and $\Delta_r G$ obtained result from the reaction (*E*)-1-Benzylidene-2,2-diphenylhydrazine + $\text{CH}_3\text{-CH}_3 \rightarrow$ (*E*)-1-(α,β -dimethylbenzylidene)-2,2-diphenylhydrazine + H_2 . The formation values were calculated from $\Delta_f H$ ($\text{C}_{21}\text{H}_{20}\text{N}_2$, 298K) and $\Delta_f G$ ($\text{C}_{21}\text{H}_{20}\text{N}_2$, 298K). From the Table I it is observed that the lowest reaction and formation ΔG values, are for the molecules in Figure 1 (A216) ($\Delta_r G=10.76$ and $\Delta_f G=-199.15$) and for (A213) ($\Delta_r G=12.92$ Kcal/mol and $\Delta_f G=-197.38$). The highest ΔG values are for (A214) ($\Delta_r G=18.98$ and $\Delta_f G= -196.43$). The same trend is observed

Table I. Theoretically calculated values of the thermochemical properties of reaction and formation, standard enthalpy $\Delta_r H$, $\Delta_f H$ and Gibbs free energy $\Delta_r G$, $\Delta_f G$, total energies and Zero-Point Vibrational Energies of the modeled isomers of Figure 1. Enthalpies, Gibbs free energy and ZPVE are in (Kcal/mol) at T=298.15 K and pressure 1 atm, for each $A20 + CH_3-CH_3 \rightarrow A21N + H_2$.

Molecule	$D_r G$ (Kcal/mol)	$D_r H$	$D_f G$	$D_f H$	E (Hartree)	ZPVE (Kcal/mol)
A211	16.46	13.34	-196.54	179.38	-921.98702	221.864
A212	13.54	10.97	-198.37	177.00	-921.99065	221.636
A213	12.92	11.15	-197.38	177.19	-921.99038	221.627
A214	18.98	14.65	-196.43	180.69	-921.98516	222.249
A215	13.15	9.64	-200.62	175.68	-921.99271	221.774
A216	10.76	9.18	-199.15	175.22	-921.99329	221.344

Table II. 1H NMR and ^{13}C chemical shifts of the atoms in Figure 2, for molecules A211, A212, A213, A214, A215, A216 theoretical obtained using $(CD_3)_2CO$ and the B3LYP/6-311+G(d,p) GIAO method and A215 (Mendoza et al. 2011) and A20 (Mendoza et al. 2012) experimental.

Molecules	C_1 (ppm)	C_2	C_7	C_{16}	C_{17}	H_3	H_2	H_1
A20	145.5	143.2	137.8	-	-	6.82	6.08	-
A20 exp	143.7	136.3	135.2	-	-	7.36	7.28	-
A211	154.6	140.9	136.1	14.1	22.5	7.25	6.1	1.9
A212	154.1	138.1	135.4	19.7	21.3	7.08	7.0	1.7
A213	154.1	140.0	135.5	19.0	21.4	7.06	6.0	2.1
A214	154.2	136.9	139.6	21.0	28.9	7.59	6.1	2.4
A215	154.2	141.5	138.1	20.6	20.9	6.78	6.0	2.0
A215 exp	143.83	136.72	136.56	18.81	18.91	7.35	7.10	2.23
A216	154.1	142.7	138.7	21.9	21.7	6.74	6.0	2.1

for $\Delta_r H$ and $\Delta_f H$ the lowest values for A213 and A216, the highest value is for A214 the molecule with the highest repulsion between methyl groups. Likewise, the total Hartree energy of each molecule shows a similar behavior to the thermodynamic properties, with lower values for A213 and A216, higher value for A214. From Table I it is observed that each molecule has unique values of energy and thermochemical quantities, the Gibbs free energy ΔG decreases when methyl is at α and β moves away when

the electrostatic repulsion between the methyl groups is reduced, and ΔG increases when the repulsion between the methyl groups increases when they are approached. This indicated a less stability of A214 which can be reflected in a most difficult molecule to obtain. Total energy of each isomer reveal A216 is the most stable, and the ZPVE likewise the lowest value is for isomer A216. The highest values for total energy and ZPVE are for isomer A214.

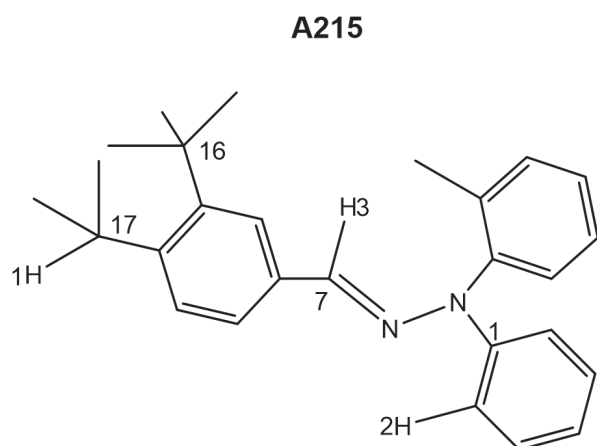


Figure 2. Molecule (E)-1-(3,4- Dimethylbenzylidene)-2,2-diphenylhydrazine (215) where is shown carbon and hydrogen atoms for theoretical calculations of NMR chemical shifts.

¹³C NMR chemical shifts.

To simplify the reading, Figure 2 shows the labeling of hydrogen and carbon atoms in the A215 isomer, where the carbon atom (C_7) and the hydrogen atom (H_3) are in the H-C=N-N hydrazone functional group. In addition are analyzed ¹³C-NMR chemical shifts over these C atoms

(C_1 , C_2 , C_7 , C_{16} , C_{17}). In principle, these are more affected by the induced magnetic field than the further away hydrogen (H_1 , H_2) atoms. From Table I and Table II it is observed the thermodynamic values to be related to ¹H and ¹³C NMR chemical shifts at H_1 , H_3 and C_7 of the structure in Figure 2. H_1 is on one of the dimethylbenzylidene methyls meanwhile H_3 , C_7 are on the hydrazone functional group H-C=N-N. The ¹³C NMR chemical shift of C_7 shows the lowest values for A212 and A213, the highest value is for A214. Comparison of the behavior of thermodynamic properties and chemical shift of H_1 , H_3 and ¹³C NMR protons of C_7 from Table II is presented in Figure 3, Figure 4 and Figure 5, which behave similarly with thermodynamic properties $\Delta_f G$, $\Delta_f G$, $\Delta_f H$ and $\Delta_f H$. Data calculated in this work and experimental ¹³C NMR data of C=N in hydrazones are compared. They have been reported (Gordon et al. 1984), where chemical shift values varying between 135-139 ppm depending on the substituents are presented. The phenylhydrazones in (Patorski et al. 2013) presented data for ¹³C NMR in the

Table III. IR signals using the B3LYP method (Becke 1993, Alecu et al. 2010) with 6-311++G(d,p) were obtained for the molecules in Figure 1. Experimental, uncorrected vibrational frequencies of A215 (Mendoza et al. 2011) and A20 (Mendoza et al. 2012) values in cm^{-1} .

Molecules	$\nu(\text{C-H})_{\text{asym}}$	$\nu(\text{C-H})_{\text{sym}}$	$\nu(\text{C=N})$	$\nu(\text{CN-N})$	UV λ_{max} (nm)
A20	3166.87	3167.19	1573.53	1214.79	348.34
A20 exp			1586, 1490		340.13
A211	3188.33	3169.27	1638.47 - 1607.83	1231.33	348.34
A212	3188.44	3168.40	1632.68 - 1592.62	1246.08	362.65
A213	3188.52	3169.54	1632.39 - 1600.61	1231.72	359.48
A214	3188.83	3169.38	1637.72 - 1596.29	1245.68	358.81
A215	3188.25	3168.07	1637.43 - 1596.70	1237.00	359.87
A215 exp	3033.00	2933.00	1588, 1490	1221.00	341.24
A216	3188.55	3168.63	1625.84 - 1613.21	1234.63	356.78

range of 139.28 - 145.28 ppm. (Neuvonen et al. 2003) reported ^{13}C signal for C=N at 125.78 MHz, which is shielded with increasing electron density on carbon, in the range of 135.8 - 140.4 ppm for molecules similar to this report. It has been reported (Öncü-Can et al. 2017) have reported the synthesis and characterization of hydrazones exhibiting ^{13}C NMR signals at 75 MHz shift for C=N around 137.19 ppm, 137.55, 137.56.43 etc., depending on the substituents. It has been reported (Meléndrez-Luévano et al. 2013) report the molecule (E)-1-(2,4-dinitrobenzylidene)-2,2-diphenylhydrazine, with shift at 135.02 ppm ^{13}C NMR (400 MHz, $(\text{CD}_3)_2\text{CO}$) for C=N. In reference (Mendoza et al. 2012) the shift for C=N is 135.72 ppm at 400 MHz in $(\text{CD}_3)_2\text{CO}$, for molecule A20 in Figure 1. In (Mendoza et al. 2011) the experimental molecule A215 in Figure 1, shows ^{13}C NMR signal at 400 MHz in $(\text{CD}_3)_2\text{CO}$, at 135.18 ppm. From experimental data it is observed in (Meléndrez-Luévano et al. 2013) that the C=N signal is at high fields, assuming that C_7 is shielded due to the inductive effect of the NO_2 groups of the benzylidene, so that C_7 has less nucleophilic

character. In (Gomes et al. 2019, Arsenyev et al. 2016) the reported molecules have ^{13}C NMR signals for C=N at high fields, due to the methyl groups in the benzylidene, indicating that the carbon atom has more charge density and less nucleophilic character. Figure 2 shows the C atoms in the A215 molecule generating ^{13}C NMR signals; experimental NMR chemical shifts of C_7 (A215) are from (Mendoza et al. 2011), theoretical calculations are shown in Table II for A211, A212, A213, A214, A215 and A216. The molecule with the most unprotected C in C=N, theoretically calculated is A214, since its signal is presented at low fields, assuming it has higher electron density so the C_7 carbon atom in C=N has less nucleophilic character. The most nucleophilic character in C=N is for A212, which is more shielded. It seems that resonance and inductive effects are responsible for the protection. The experimental molecule A215 has ^{13}C NMR 135.18 ppm at the high field than A215 theoretically calculated (138.079 ppm), some authors use a scale factor of 0.96 (Pierens 2014).

Table IV. Bond distances and Mulliken charges of the C and H atoms of the imine group of Figure 2. Mulliken charge number of electron. Distances in Å. For experimental A215 (Mendoza et al. 2011) and A20 (Mendoza et al. 2012), and theoretical calculated.

Molecules	N=C (Å)	N-N (Å)	H-CN	Mulliken charge C_7	Mulliken charge H_3
A20	1.28	1.3572	1.09	-0.154	---
A20 exp	1.279	1.3689	0.93	---	---
A211	1.287714	1.35822	1.08700	-0.324	-0.015
A212	1.28797	1.35262	1.08773	-0.438	0.016
A213	1.28779	1.35814	1.08770	-0.361	0.032
A214	1.29033	1.36186	1.08629	-0.462	-0.034
A215	1.28581	1.35956	1.09117	-0.167	0.101
A215 exp.	1.2773	1.3765	0.9300	---	---
A216	1.28589	1.35873	1.09105	-0.197	0.130

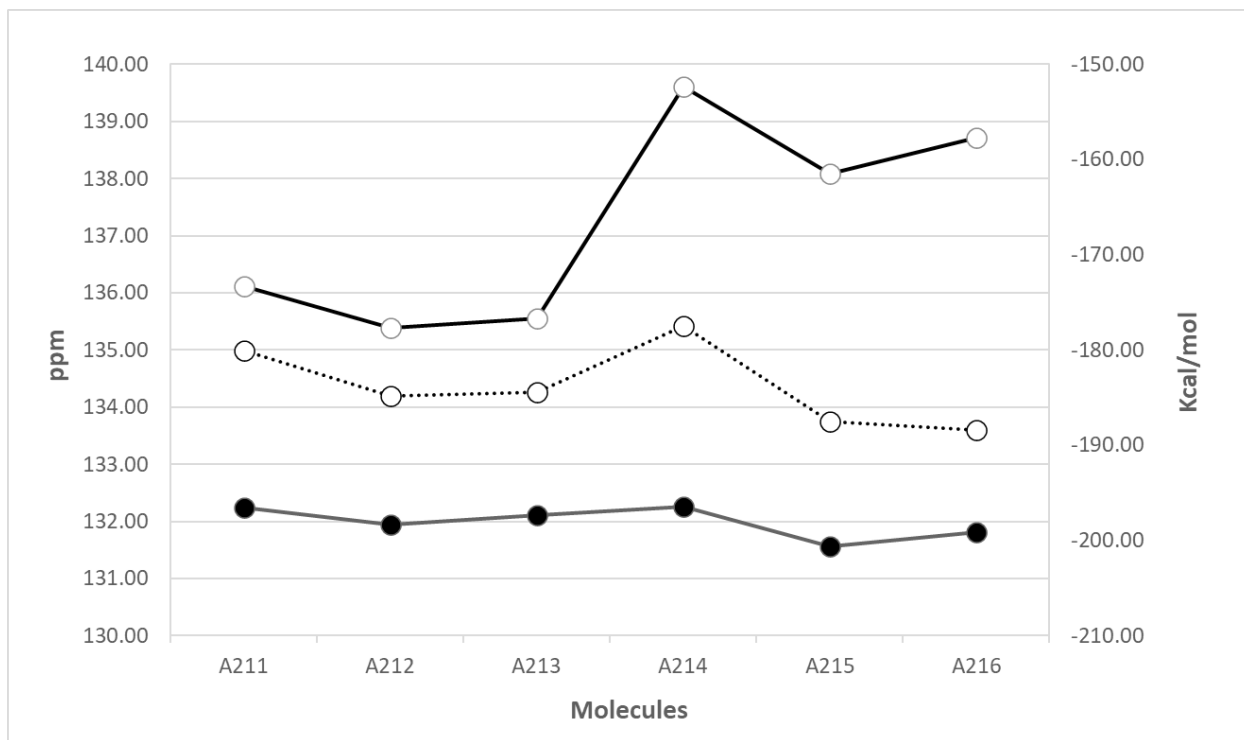


Figure 3. Comparison of the behavior of ^{13}C NMR chemical shifts for C_7 of figure 2 (solid line empty circles), with thermodynamic properties Gibbs free energy of formation $\Delta_f G$ (solid line black circles) and Gibbs free energy of reaction $\Delta_r G$ (dashed line empty circles) for (E)-1-(α,β -Dimethylbenzylidene)-2,2-diphenylhydrazine isomers of Figure 1.

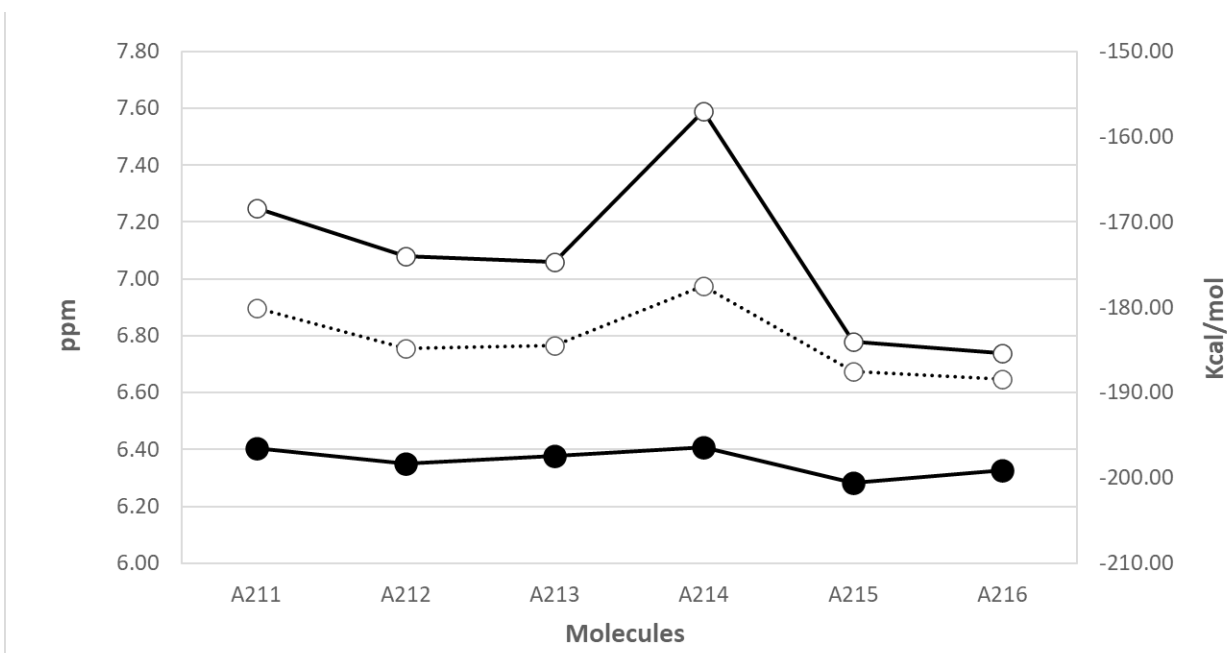


Figure 4. Comparison of ^1H NMR chemical shift behavior for the H_3 of Figure 2 (solid line of empty circles), thermodynamic properties Gibbs free energy of formation $\Delta_f G$ (solid line of black circles) and Gibbs free energy of reaction $\Delta_r G$ (dashed line of empty circles) for (E)-1-(α,β -Dimethylbenzylidene)-2,2-diphenylhydrazine isomers of Figure 1.

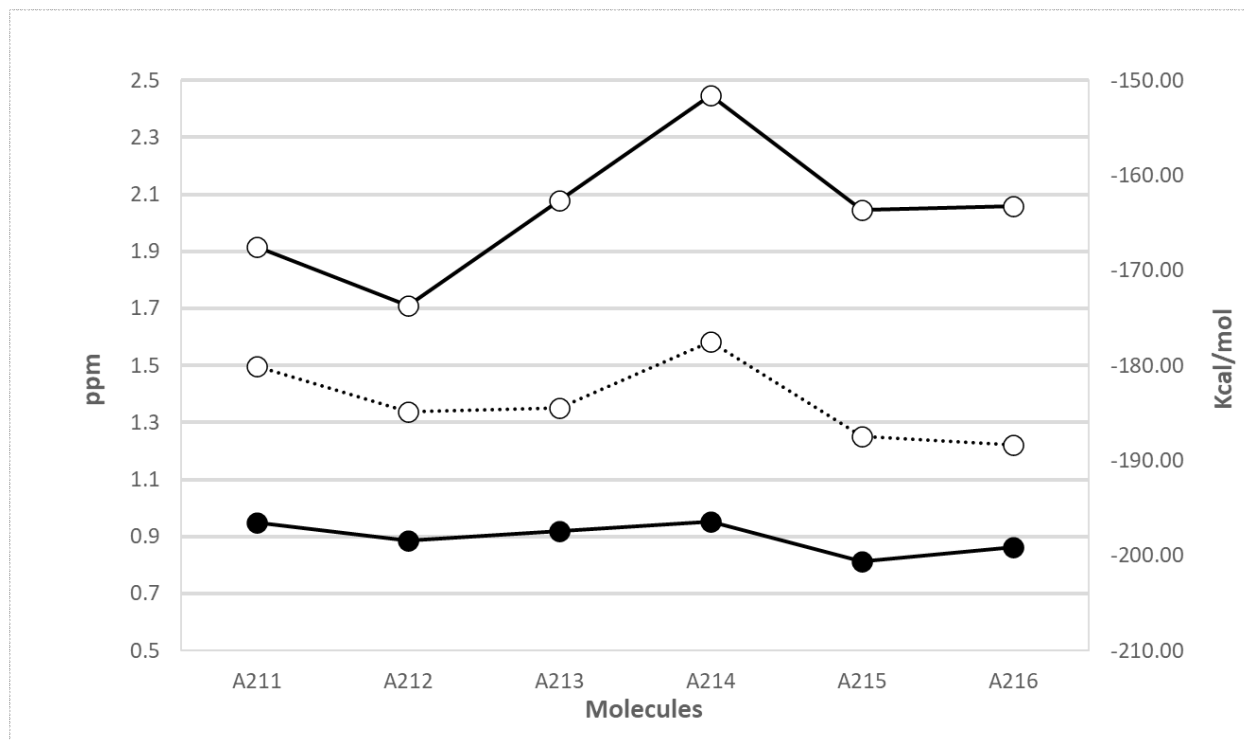


Figure 5. Comparison of the behavior of ^1H NMR chemical shifts for H_1 of figure 2 (solid line empty circles), thermodynamic properties Gibbs free energy of formation $\Delta_f G$ (solid line black circles) and Gibbs free energy of reaction $\Delta_r G$ (dashed line empty circles) for (E)-1-(α,β -Dimethylbenzylidene)-2,2-diphenylhydrazine isomers of Figure 1.

^1H NMR chemical shifts

Likewise, data calculated here and reported experimental data of ^1H NMR signals for the H_3 proton of $\text{HC}=\text{N}$ in Figure 2 are compared. Some reports such as (Flores-Alamo et al. 2014) show a shift of 7.60 ppm, at 400 MHz using $(\text{CD}_3)_2\text{CO}$, for $\text{HC}=\text{N}$ in the molecule of (E)-1-(2-nitrobenzylidene)-2,2-diphenylhydrazine. Also (Higgs et al. 2019) reported ^1H NMR for $\text{HC}=\text{N}$ at 8.81-8.64 ppm, at 400 MHz using D_2O for N,N,N-trimethyl-2-oxo-2-(2-(quinolin-8-ylmethylene)hydrazinyl)ethane-1-aminium, for the 2-(2-(2-hydroxybenzylidene)hydrazinyl)-N,N,N-trimethyl-2-oxoethane-1-aminium molecule, a signal from 8.12 to 7.95. It is observed that the signal of the proton in the second molecule is located in high fields, which means that the proton is protected and has little acidic character, according to the substituents in the molecules.

In (Toledano-Magaña et al. 2015) has reported new compounds and characterized them using ^1H NMR signals at 400 MHz in $(\text{CD}_3)_2\text{CO}$ of some hydrazones such as (E)-1-(2-Nitrobenzylidene)-2-phenylhydrazine, 8.23 ppm (s, 1H, C=N), for (E)-1-(3-nitrobenzylidene)-2-phenylhydrazine, 7.85 (s, 1H, C=N), (E)-1-(4-nitrobenzylidene)-2-phenylhydrazine 7.94 (s, 1H, C=N) and 8.63 ppm for (E)-1-(2,4-dinitrobenzylidene)-2-phenylhydrazine. From the chemical shifts, it is observed that the signals at low fields are 8.63 and 8.23, indicating that these protons are poorly shielded. The signals at high fields are 7.94 and 7.85 ppm, indicating that the proton at 7.85 is shielded with little acidic character. Figure 2 and Table II show the H atoms whose NMR proton signals are theoretically calculated in molecules A211, A212, A213, A214, A214, A215 and A216 the experimental chemical shifts for A215 were reported in (Mendoza et al. 2011). From

the calculated chemical shifts it is observed that A216 has the most shielded H₃ proton (6.74 ppm). The most unshielded proton is A214 (7.59 ppm), which could be considered the most acidic proton. The experimental signal of A215 at 7.37 ppm, is at high fields and the theoretical value of A215 6.78 ppm. The experimental value at A215 of the methyl H₁ proton of methylbenzylidene is in low fields, the H of diphenylhydrazine H₁, H₂ are in high fields and H of H-C=N in low fields, which means that the H₃ has less acidic character in the molecule. The same trend is observed for the theoretically calculated molecules. These data indicate a trend of experimental molecules that is repeated in the theoretical data.

Vibrational Spectra and bond distances

Seeking to validate the theoretical calculations of the vibrational spectra, the data obtained are compared with previously reported experimental data. Table III reports the experimental IR frequencies of A20 (Mendoza et al. 2012) A215 (Mendoza et al. 2011) and also shows the theoretical values of A20, A211, A212, A213, A214, A215 and A216. In Table IV are reported C=N, N-N, H-CN distances of molecules of Figure 1. Some authors such as (Tosi et al. 1988), reported experimental results of IR spectra of benzaldehyde methyl (phenyl) hydrazone, the normal mode of stretching vibration for (C = N) appears at 1555 to 1570 cm⁻¹, depending on the substituents. The C=N bond distance is 1.29 Å and H-CN, 1.12 (Arsenyev et al. 2016) reported experimental IR signals of 4,6-di-*t*-butyl-3-((diphenylhydrazono)methyl) benzene-1,2-diol, where the band (C=N) is observed at 1593 - 1600 cm⁻¹; a C=N distance of 1.29 Å and an H-CN distance of 0.97 Å. Data for another similar structure, 4-{2-[(pyren-1-yl) methylidene] hydrazinyl}benzonitrile, reported by (Ghosh et al. 2017), show experimental IR signals for (C=N) at 1610 cm⁻¹, a C=N distance of 1.27 Å and an

H-CN distance of 0.93 Å. (Mendoza et al. 2012) reported for the signal of (E)-1-benzylidene-2,2-diphenylhydrazine $\nu(\text{C}=\text{N})$ at 1586-1490 cm⁻¹, a distance of 1.279 Å and H-CN 0.93 Å. (Mendoza et al. 2011) presented experimental IR signals for (E)-1-(3,4-Dimethylbenzylidene)-2,2-diphenylhydrazine, a hydrazine with two methyl groups where the influence of substituents on the experimental values is observed, for $\nu(\text{C}=\text{N})$ 1588, 1490 cm⁻¹ and C=N distance of 1.2773 Å and H-CN distance of 0.93 Å. (Mendoza et al. 2012) reported experimental IR signals for (E)-1-(2,4-dinitrobenzylidene)-2,2-diphenylhydrazine, $\nu(\text{C}-\text{H})$ 3119 cm⁻¹ and $\nu(\text{C}=\text{N})$ 1600 cm⁻¹, C=N distance of 1.288 Å and H-CN distance of 0.93 Å. It is observed that for experimental molecules in (Jacquemin et al. 2008, Mendoza et al. 2011, Meléndrez-Luévano et al. 2013) the IR signal for $\nu(\text{C}=\text{N})$ is related to the distance, indicating a variation in the character of the double bond. The C=N distance increases when the inductive effect of methyl groups is in the structure, and the effect increases when NO₂ groups are present. In (Tosi et al. 1988, Ghosh et al. 2017) the H-CN distance varies, making H acidic. As the IR signal increases, the theoretically calculated H-C distance increases. For the molecules in Table IV, it is observed that the position of the methyl groups changes the IR signal of the $\nu(\text{C}=\text{N})$ group.

Theoretical and Experimental Structural Parameters

Comparing the structural parameters, theoretically calculated and some experimental distances, it is observed that the C=N distance varies by changing the character of the double bond, the hydrogen in H-CN becoming more acidic as the bond distance increases. For example, in the molecule (A214), the two methyl groups have an inductive effect that lengthens the C=N bond distance and makes the hydrogen in H-CN less acidic. The shorter C=N distance

belongs to the molecule (A215) and the larger H-CN distance. Table IV shows the experimental distance values of (Mendoza et al. 2011) (A215) N=C (1.2773 Å) and N-N (1.3765 Å). The theoretical values for the same molecule are N=C (1.28581 Å) and N-N (1.35956 Å). Several hydrazine molecules (Mendoza et al. 2011, Meléndrez-Luévano et al. 2013, Jasinski et al. 2012, Toledano-Magaña et al. 2014, Ji et al. 2010) have been reported with similar C=N (1.266 to 1.288) and N-N (from 1.3534 to 1.4103) distances. The C=N distance increases as the negative charge of C on the C=N imine becomes larger. The distance in a double bond is related to the electronic localization (Nigst et al. 2012), which causes C to have a larger negative atomic charge, and C increases its nucleophilicity. The position of the methyl groups on (A213) causes the imine carbon to have a higher partial negative charge, and hydrazine with 3,4-dimethylbenzylidene (A214) produces the lowest negative charge on the C imine. The inductive effect causes the C imine to acquire a negative charge when methyl is on the benzylidene near C₁. Thus, the C of C=N varies its reactivity to increase the nucleophilic character as the distance increases. The N-N region of the molecule shows no clear trend in geometry or reactivity, despite the effect (Nigst et al. 2012), where methylation increases the nucleophilicity of the imine carbon atom. In Table III, the experimental UV values reported in references (Mendoza et al. 2012) $\lambda_{\text{max}} = 340.13$ nm for the molecule (E)-1-Benzylidene-2,2-diphenylhydrazine and (Mendoza et al. 2011) $\lambda_{\text{max}} = 341.24$ nm for the molecule (3,4-Dimethylbenzylidene)-2,2-diphenylhydrazine and UV $\lambda_{\text{max}} = 443.36$ nm for (E)-1-(2,4-dinitrobenzylidene)-2,2-diphenylhydrazine (Meléndrez-Luévano et al. 2013), suggest that the latter molecule is more reactive. Theoretical UV λ_{max} wavelengths (Bharanidharan et al. 2017, Torje et al. 2012)

are presented for the molecules in Figure 1. Although all molecules are isoelectronic and vary only in the position of the dimethyl groups on the benzylidene, all UV λ_{max} are different. This indicates that the n \rightarrow π^* transition varies with energy, this signal occurs around 350 nm (Jacquemin et al. 2008). It is assumed that A212 has the highest feasibility to react globally and A211 the lowest, among the modeled molecules. The UV λ_{max} value for the experimental and modeled A215 molecule deviates by 5.5 % (Weishaar et al. 2003).

Electrostatic Potential and Dipole Moment

Figure 6 shows the theoretically calculated molecular electrostatic potential (Shin & Jung 2022) and dipole moment vector for (E)-1-(α , β -Dimethylbenzylidene)-2,2-diphenylhydrazine molecules likewise, the Mulliken charges (e) of each atom of each molecule were calculated. The Mulliken charges of the H atom of the HC=N-N group are reported in Table IV, because it is the atom that changes with the value of the electrostatic potential, there was used Mulliken charges and MEP analyses to find reactive sites in the modeled isomers (Rameshkumar & Santhi 2018). The values obtained are compared with the various previous theoretical calculations of the electrostatic potential, such as (Murray et al. 1990, Shin & Jung 2022) who has obtained MEP to study hydrazine and derivatives to correlate with binding forces, or (Monasterios et al. 2006) who used MEP to correlate with antibacterial activity. The MEP reflects at any point the electron density and also the contributions of all nuclei and electrons in the molecule (Murray & Politzer 2011). The calculated electrostatic potential of the molecules in Figure 1 shows positive regions on the H₃ atom in Figure 2, the Mulliken charges are in Table IV for H₃ are -0.015 for A211, 0.016 for A212, 0.32 for A213, -0.034 for A214, 0.101 for A215 and 0.130 for A216. It is observed in Figure

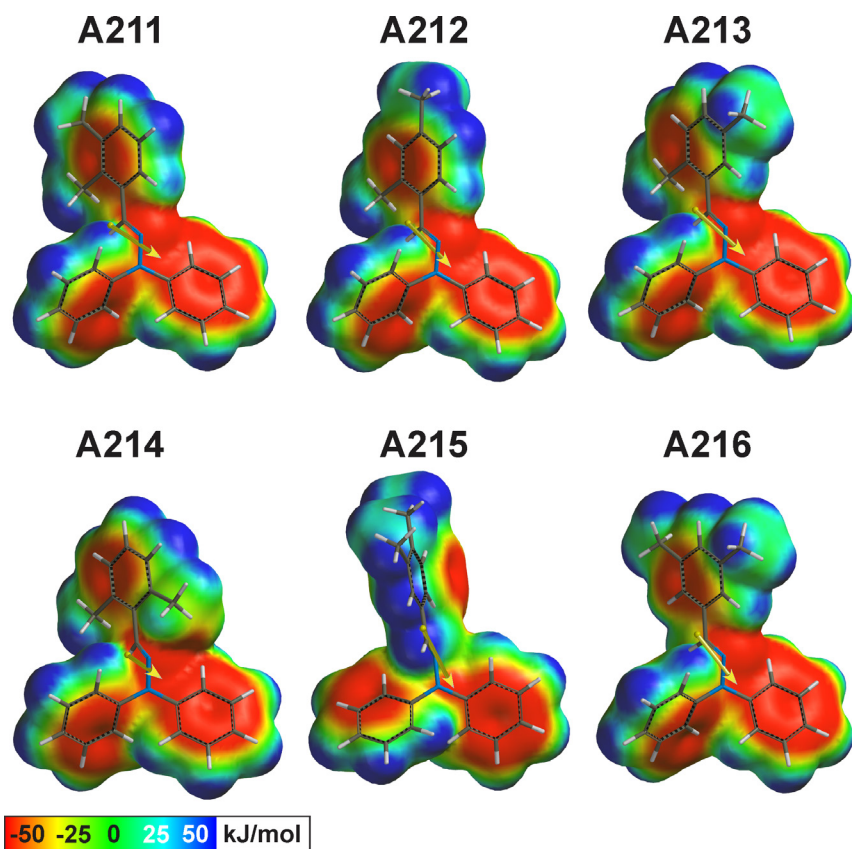


Figure 6. Molecular electrostatic potential for (E)-1-(α,β-Dimethylbenzylidene)-2,2-diphenylhydrazine isomers. Red areas represent negative regions (-50 KJ/mol), blue represent positive regions (50 KJ/mol).

6, that the electrostatic potential varies as the methyl groups change position, also regions of positive and negative potential are observed through which attractive interactions can occur, and a significant positive region is found at the H_3 in A214 molecules, which also coincide with the lowest Mulliken charge, as used previously (Santamaria et al. 1998).

CONCLUSIONS

From the theoretically calculated thermochemical data $\Delta_f G$ $\Delta_f H$ $\Delta_f G$ $\Delta_f H$ of Table I, it was possible to identify the most stable conformers. The molecule (E)-1-(2,6-dimethylbenzylidene)-2,2-diphenylhydrazine (A214) has the highest values as well as the total energy, likewise the values of 1H and ^{13}C chemical shifts for H_3 and C_7 of the hydrazine group $H-C=NN$ (Table II) and $C=N$ distance obtained computationally

(Table IV), this implies it is the most difficult molecule to obtain theoretically. From Table I it is observed that the enthalpy and Gibbs free energy of formation increase when the methyl groups are neighbors of the hydrazine group and the values decrease as the methyls move away from $C=N$. From the ^{13}C NMR data it was observed that the chemical shift for C_7 has the most nucleophilic C character of $C=N$ for A214. From the 1H NMR the protected protons are observed and used to predict possible reactivity properties, the chemical shifts of H_3 and C_7 and the thermochemical properties such as Gibbs free energy and Enthalpy, present the same trend in the molecules studied. From the IR data it was observed the position of $\nu(C=N)$ and the experimental distances to be related. It is possible to relate the IR data to the double bond character of $C=N$. The Mulliken charge and H_3 MEP of the molecules also agree with the

trends of the thermodynamic properties, the ^{13}C , ^1H chemical shift.

Acknowledgments

The authors gratefully acknowledge the computing time granted by LANCAD and CONACYT on the supercomputer Yoltla at the LSVP at UAM-Iztapalapa. Thanks to VIEP-BUAP for the sponsorship of this project RAGJ-NAT 2018 00614.

REFERENCES

- ALECU IM, ZHENG J, ZHAO Y & TRUHLAR DG. 2010. Computational Thermochemistry: Scale Factor Databases and Scale Factors for Vibrational Frequencies Obtained from Electronic Model Chemistries. *J Chem Theory Comput* 6: 2872-2887.
- ANDERSSON MP & UVDAL P. 2005. New Scale Factors for Harmonic Vibrational Frequencies Using the B3LYP Density Functional Method with the Triple-zeta Basis Set 6-311+G(d,p). *J Phys Chem A* 109: 2937-2941.
- ARSENYEV MV, KHAMALETDINOVA NM, BARANOV EV, CHESNOKOV SA & CHERKASOV VK. 2016. Synthesis, structures, and properties of new sterically hindered hydrazine-based catecholaldimines. *Russ Chem Bull* 65: 1805-1813.
- ARSHAD MN, BIBI A, MAHMOOD T, ASIRI AM & AYUB K. 2015. Synthesis, Crystal Structures and Spectroscopic Properties of Triazine-Based Hydrazone Derivatives; A Comparative Experimental-Theoretical Study. *Molecules* 20: 5851-5874.
- ATKINS P, PAULA JD & KEELER J. 2018. *Physical Chemistry*. New York: Oxford University Press, New York, USA, p. 532-536.
- BALAKIT AA, MAKKI SQ, SERT Y, UCUN F, ALSHAMMARI MB, THORDARSON P & EL-HITI GA. 2020. Synthesis, spectrophotometric and DFT studies of new Triazole Schiff bases as selective naked-eye sensors for acetate anion. *Supramol Chem* 32: 519-526.
- BAUERFELDT GF, ARBILLA G & SILVA EC. 2005. Evaluation of Reaction Thermochemistry Using DFT Calculated Molecular Properties: Application to trans-HONO (X1A') \rightarrow HO(X2P) + NO(X2P). *J Braz Chem Soc* 16: 190-196.
- BECKE AD. 1993. A new mixing of Hartree-Fock and local density-functional theories. *J Chem Phys* 98: 1372-1377.
- BENASSI R, FERRARI E, LAZZARI S, SPAGNOLO F & SALADINI M. 2008. Theoretical study on Curcumin: A comparison of calculated spectroscopic properties with NMR, UV-Vis and IR experimental data. *J Mol Struct* 892: 168-176.
- BHARANIDHARAN S, SALEEM H, SUBASHCHANDRABOSE S, SURESH M & RAMESH BN. 2017. FT-IR, FT-Raman and UV-Visible Spectral Analysis on (E)-N'-(thiophen-2-ylmethylene) Nicotinohydrazide. *Arch Chem Res* 1: 1-7.
- BOHN MA & KLAPOTKE TM. 2004. DFT and G2MP2 Calculations of the N-N Bond Dissociation Enthalpies and Enthalpies of Formation of Hydrazine, Monomethylhydrazine and Symmetrical and Unsymmetrical Dimethylhydrazine. *Z Naturforsch* 59b: 148-152.
- CANCÉS E, MENNUCCI B & TOMASI J. 1997. A new integral equation formalism for the polarizable continuum model: Theoretical background and applications to isotropic and anisotropic dielectrics. *J Chem Phys* 107: 3032-3041.
- CURTISS LA, RAGHAVACHARI K, REDFERN PC & POPLE JA. 1997. Investigation of the use of B3LYP zero-point energies and geometries in the calculation of enthalpies of formation. *Chem Phys Lett* 270: 419-426.
- DEGE N, GÖKCE H, DOĞAN OE, ALPASLAN G, AĞAR T, MUTHU S & SERT Y. 2022. Quantum computational, spectroscopic investigations on N-(2-((2-chloro-4,5-dicyanophenyl) amino)ethyl)-4-methylbenzenesulfonamide by DFT/TD-DFT with different solvents, molecular docking and drug-likeness researches. *Colloid Surf A* 638: 128311.
- ELIEL EL. 1960. Conformational Analysis in Mobile. *J Chem Educ* 37: 126-133.
- ELIEL EL & MARTIN RJ. 1968. Conformational Analysis XIII. The validity of the nuclear magnetic of establishing conformational equilibria. *J Am Chem Soc* 90: 682-689.
- FLORES-ALAMO M, MELENDREZ LUEVANO R, ORTIZ-MÁRQUEZ JA, SANSINENEA-ROYANO E & CABRERA-VIVAS BM. 2014. Crystal structure of (E)-1-(2-nitrobenzylidene)-2,2-diphenylhydrazine. *Acta Cryst E70*: o909-o910.
- FRISCH MJ, TRUCKS GW & CHEESEMAN JR. 1996. Systematic Model Chemistries Based on Density Functional Theory: Comparison with traditional Models and with Experiment: In: *Recent Developments and Applications of Modern Density Functional Theory Theoretical and Computational Chemistry*. Vol. 4. Netherlands: Elsevier, p. 679.
- FRISCH MJ ET AL. 2016. *Gaussian 09 Revision A.02*. Wallingford CT: Gaussian Inc.
- GHOSH P, PAUL S & BANERJEE P. 2017. How explosive TNP interacts with a small tritopic receptor: a combined crystallographic and thermodynamic approach. *CrystEngComm* 19: 6703-6710.
- GÖKCE H, ŞEN F, SERT Y, ABDEL-WAHAB B, KARIUKI B & EL-HITI G. 2022. Quantum Computational

- Investigation of (E)-1-(4-methoxyphenyl)-5-methyl-N'-(3-phenoxybenzylidene)-1H-1,2,3-triazole-4-carbohydrazide. *Molecules* 27: 2193.
- GOMES LR ET AL. 2019. Crystal structures and Hirshfeld surface analysis of four 1,4-bis(methoxyphenyl)-2,3-diazabuta-1,3-dienes: comparisons of the intermolecular interactions in related compounds. *Z Kristallogr* 234: 59-71.
- GORDON MS, SOJKA SA & KRAUSE JG. 1984. Carbon-13 NMR of Para-Substituted Hydrazones, Phenylhydrazones, Oximes, and Oxime Methyl Ethers: Substituent Effects on the Iminyl Carbon. *J Org. Chem* 49: 97-100.
- HAMZEHLIOUEIAN M. 2017. A density functional theory study on the reaction mechanism of hydrazones with α -oxo-ketenes: Comparison between stepwise 1,3-dipolar cycloaddition and Diels–Alder pathways. *Comptes Rendus Chimie* 20: 508-519.
- HANSON RK, SPEARRIN RM & GOLDSTEIN CS. 2016. *Spectroscopy and Optical Diagnosis for Gases*. Vol. 1. Switzerland: Springer International Publishing, p. 79-89.
- HARESS NG, GOVINDARAJAN M, AL-WABLI RI, ALMUTAIRI MS, AL-ALSHAIKH MA, AL-SAADY AA & ATTIA MI. 2016. Spectroscopic (FT-IR, FT-Raman, UV, 1H and 13C NMR) profiling and theoretical calculations of (2E)-2-[3-(1H-imidazol-1-yl)-1-phenylpropylidene] hydrazinecarboxamide: An anticonvulsant agent. *J Mol Struct* 1118: 219-232.
- HIGGS PL, RUI-SANCHEZ AJ, DALMINA M, HORROCKS BR, LEACH AG & FULTON DA. 2019. Enhancing the Kinetics of Hydrazone Exchange Processes: An Experimental and Computational Study. *Org Biomol Chem* 17: 3218-3224.
- JACQUEMIN D, PERPÈTE EA, SCUSERIA GE, CIOFINI I & ADAMO C. 2008. TD-DFT Performance for the Visible Absorption Spectra of Organic Dyes: Conventional versus Long-Range Hybrids. *J Chem Theory Comput* 4: 123-135.
- JASINSKI JP, GOLEN JA, PRAVEEN AS, NARAYANA B & YATHIRAJAN HS. 2012. 1,2-Bis(3-phenoxybenzylidene)hydrazine. *Acta Cryst E* 68: o81.
- JESCHKE G. 2015. *Advanced Physical Chemistry. Statical Thermodynamics*. G. Jeschke Ed. Zürich: Swiss Federal Institute Hochschule, p. 31-39.
- JI NN, SHI ZQ, ZHAO RG, ZHENG ZB & LI ZF. 2010. Synthesis, Crystal Structure and Quantum Chemistry of a Novel Schiff Base N-(2,4-Dinitro-phenyl)-N'-(1-phenylethylidene)-hydrazine. *Bull Korean Chem Soc* 31: 881-886.
- JUARISTI E & MUÑOZ-MUÑIZ O. 2001. Enthalpic and Entropic Contributions to the Conformational Free Energy Differences in Monosubstituted Cyclohexanes. *Rev Soc Quím Méx* 45: 218-224.
- KRISHNAN VV. 2019. Molecular Thermodynamics Using Magnetic Resonance (NMR). *Inventions* 4: 1-15.
- LANDERVILLE AC, CONROY MW, BUDZEVICH MM, LIN Y, WHIT CT & OLEYNIK II. 2010. Equations of state for energetic materials from density functional theory with van der Waals, thermal, and zero-point energy corrections. *Appl Phys Lett* 97: 251908.
- LEE C & SOSA C. 1994. Local density component of the Lee–Yang–Parr correlation energy functional. *J Chem Phys* 100: 9018-9024.
- MELÉNDREZ-LUÉVANO R, CABRERA-VIVAS BM, FLORES-ALAMO M, RAMÍREZ JC & CONDE-SÁNCHEZ P. 2013. (E)-1-(2,4-Dinitrobenzylidene)-2,2-diphenylhydrazine. *Acta Cryst E* 69: o1039.
- MENDOZA A, CABRERA VIVAS BM, MELENDREZ LUEVANO R, RAMÍREZ JC & FLORES-ÁLAMOS M. 2011. (E)-1-(3,4-Dimethylbenzylidene)-2,2-diphenylhydrazine. *Acta Cryst E* 67: o1287.
- MENDOZA A, MELENDREZ-LUEVANO R, CABRERA-VIVAS BM, LOZANO-MARQUEZ CD & CARRANZA V. 2012. (E)-1-Benzylidene-2,2-diphenylhydrazine. *Acta Cryst E* 68: 0434.
- MERRICK JP, MORAN D & RADOM L. 2007. An Evaluation of Harmonic Vibrational Frequency Scale Factors. *J Phys Chem A* 111: 11683-11700.
- MONASTERIOS M, AVENDAÑO M, AMARO MI, INFANTE W & CHARRIS J. 2006. Relation between molecular electrostatic potential, several electronic properties and antibacterial activity of some synthetic furane derivatives. *J Mol Struct* 798: 102-108.
- MURRAY JS & POLITZER P. 2011. The electrostatic potential: an overview. *WIREs Comput Mol Sci* 1: 153-163.
- MURRAY JS, SUKUMAR N, RANGANATHAN S & POLITZER P. 1990. A Computational Analysis of the Electrostatic Potentials and Relative Bond Strengths of Hydrazine and Some of Its 1, 1-Dimethyl Derivatives. *Int J Quantum Chem* 37: 611-629.
- NEUVONEN K, FULOP F, NEUVONEN H, KOCH A, KLEINPETER E & PIHLAJA K. 2003. Comparison of the Electronic Structures of Imine and Hydrazone Side-Chain Functionalities with the Aid of 13C and 15N NMR Chemical Shifts and PM3 Calculations. The Influence of C=N-Substitution on the Sensitivity to Aromatic Substitution. *J Org Chem* 68: 2151-2160.
- NGUYEN TT. 2021. 1H/13C chemical shift calculation for biaryls: DFT approaches to geometry optimization. *R Soc Open Sci* 8: 210954.

- NIGST TA, ANTIPOVA A & MAYR H. 2012. Nucleophilic Reactivities of Hydrazines and Amines: The Futile Search for the α -Effect in Hydrazine Reactivities. *J Org Chem* 7718: 8142-8155.
- OCHTERSKI JW, PETERSSON GA & WIBERG KB. 1995. A Comparison of Model Chemistries. *J Am Chem Soc* 117: 11299-11308.
- ÖNCÜ-CAN N ET AL. 2017. Synthesis of New Hydrazone Derivatives for MAO Enzymes Inhibitory Activity. *Molecules* 22: 1-19.
- PATORSKI P, WYRZYKIEWICZ E & BARTKOWIAK G. 2013. Synthesis and Conformational Assignment of N-(E)-Stilbenyloxymethylenecarbonyl-Substituted Hydrazones of Acetone and o- (m- and p-) Chloro- (nitro-) benzaldehydes using of ¹H and ¹³C NMR Spectroscopy. *J Spectrosc* 197475: 1-12.
- PIERENS GK. 2014. ¹H and ¹³C NMR Scaling Factors for the Calculation of Chemical Shifts in Commonly Used Solvents Using Density Functional Theory. *J Comput Chem* 35: 1388-1394.
- RAMESHKUMAR R & SANTHI N. 2018. Synthesis, Geometry optimization, Mulliken, MEP, HOMO-LUMO and NLO properties of 2-aryl-3-(2,6-diisopropylphenyl)thiazolidin-4-one based on DFT calculations. *World Scientific News* 91: 59-72.
- RUZSINSZKY A, ALSENOY CV & CSONKA GI. 2003. Implicit Zero-Point Vibration Energy and Thermal Corrections in Rapid Estimation of Enthalpies of Formation from Hartree-Fock Total Energy and Partial Charges. *J Phys Chem A* 107: 736-744.
- SANTAMARIA R, COCHO G, CORONA L & GONZALEZ E. 1998. Molecular electrostatic potentials and Mulliken charge populations of DNA mini-sequences. *Chem Phys* 227: 317-329.
- SCOTT AP & RADOM L. 1996. Harmonic vibrational frequencies: An evaluation of Hartree-Fock, Møller-Plesset, quadratic configuration interaction, density functional theory, and semiempirical scale factors. *J Phys Chem* 100: 16502-16513.
- SHIN D & JUNG Y. 2022. Molecular electrostatic potential as a general and versatile indicator for electronic substituent effects: statistical analysis and applications. *Phys Chem Chem Phys* 24: 25740-25752.
- SOUSA JA, SILVA PP, MACHADO AE, REIS MH, ROMANIELO LL & HORI CE. 2013. Application of computational chemistry methods to obtain thermodynamic data for hydrogen production from liquefied petroleum gas. *Braz J Chem Eng* 30: 83-93.
- SOUZA LA, SILVA HC & ALMEIDA WB. 2018. Structural Determination of Antioxidant and Anticancer Flavonoid Rutin in Solution through DFT Calculations of ¹H NMR Chemical Shifts. *ChemistryOpen* 7: 902-913.
- SU X & APRAHAMIAN I. 2014. Hydrazone-based switches, metallo-assemblies and sensors. *Chem Soc Rev* 43: 1963-1981.
- TANAK H & TOY M. 2016. Molecular structure and vibrational assignment of 1-[N-(2-pyridyl)aminomethylidene]-2(1H)-Naphthalenone by density functional theory (DFT) and ab initio Hartree-Fock (HF) calculations. *Spectrochim Acta A Mol Biomol Spectrosc* 152: 525-529.
- TOLEDANO-MAGAÑA Y ET AL. 2015. Potential Amoebicidal Activity of Hydrazone Derivatives: Synthesis, Characterization, Electrochemical Behavior, Theoretical Study and Evaluation of the Biological Activity. *Molecules* 20: 9929-9948.
- TOLEDANO-MAGAÑA Y ET AL. 2014. Synthesis, characterization and evaluation of the substituent effect on the amoebicide activity o. *Med Chem Commun* 5: 989-996.
- TORJE A, VÂLEAN AM & CRISTEA C. 2012. Phenothiazine-carboxaldehyde-hydrazone derivatives synthesis, characterization and electronic properties. *Rev Roum Chim* 57: 337-344.
- TOSI G, CARDELLINI L & BOCELLI G. 1988. Charge-Transfer Complexes of Hydrazones. VI.* Structures of Six Hydrazone Derivatives. Infrared and Structural Evidence for Substituent Effects on Charge-Transfer Interactions. *Acta Cryst B* 44, 55-63.
- VERMA G, MARELLA A, SHAQUIQUZZAMAN M, AKHAR M, ALI MR & ALAM MM. 2014. A review exploring biological activities of hydrazones. *J Pharm Bioall Sci* 6: 69-80.
- WAVEFUNCTION. 2014. Spartan'14. Irving CA: Wavefunction, Inc.
- WEISHAAR JL, AIKEN GR, BERGAMASCHI BA, FRAM MS, FUJII R & MOPPER K. 2003. Evaluation of Specific Ultraviolet Absorbance as an Indicator of the Chemical Composition and Reactivity of Dissolved Organic Carbon. *Environ Sci Technol* 37: 4702-4747.
- WILCOX CF & BAUER SH. 2003. DFT calculations of thermochemical and structural parameters of tetracyanohydrazine and related tetrasubstituted hydrazines. *J Mol Struct Theochem* 625: 1-8.
- WILCOX CF, ZHANG YX & BAUER SH. 2002. DFT calculations of the thermochemistry and structures of tetrazine derivatives. *J Energ Mater* 20: 71-92.

WOLINSKI K, HINTON JF & PULAY AP. 1990. Efficient implementation of the gauge-independent atomic orbital method for NMR chemical shift calculations. *J Am Chem Soc* 112: 8251-8260.

ZAIDI SH, HAI A & NAWAR BR. 2018. Properties and Uses of Substituted Hydrazones. *J Pharm Appl Chem* 4: 17-21.

How to cite

RAMÍREZ-GARCÍA JC, VÁZQUEZ-RAMÍREZ R, PATIÑO ME, AGUIRRE-CABRERA C, CARRANZA V & GONZÁLEZ ÁLVAREZ CM. 2023. Theoretical study of Gibbs free energy and NMR chemical shifts, of the effect of methyl substituents on the isomers of (E)-1-(α,β -Dimethylbenzyliden)-2,2-diphenylhydrazine. *An Acad Bras Cienc* 95: e20220766. DOI 10.1590/0001-3765202320220766.

*Manuscript received on December 11, 2022;
accepted for publication on February 27, 2023*

JUAN CARLOS RAMÍREZ-GARCÍA¹

<https://orcid.org/0000-0003-1351-5276>

RICARDO VÁZQUEZ-RAMÍREZ²

<https://orcid.org/0000-0002-7002-0934>

MARÍA EUGENIA PATIÑO³

<https://orcid.org/0000-0003-0565-1622>

CARLA AGUIRRE-CABRERA¹

<https://orcid.org/0009-0000-0126-9042>

VLADIMIR CARRANZA³

<https://orcid.org/0000-0003-0427-4298>

CARMEN MÁRIA GONZÁLEZ ÁLVAREZ¹

<https://orcid.org/0000-0003-4788-0220>

¹Facultad de Ciencias Químicas, Benemérita Universidad Autónoma de Puebla, Av. 14 Sur Col. San Manuel, Ciudad Universitaria, Puebla, C.P. 72592 México

²Instituto de Investigaciones Biomédicas, Universidad Nacional Autónoma de México, D.F. 04510, México

³Centro de Química, Instituto de Ciencias, Benemérita Universidad Autónoma de Puebla, Av. 14 Sur Col. Jardines de San Manuel, Ciudad Universitaria, Puebla, P.O. Box 1067, C.P. 72001 México

Correspondence to: **Juan Carlos Ramírez-García**

E-mail: juan.ramirez@correo.buap.mx

Author contributions

J. C. Ramírez-García: Conceptualization, methodology, Writing original draft. R. Vázquez-Ramírez: methodology, software modelling and visualization. Writing and review & editing. M. E. Patiño: Data curation, writing review & editing. C. Aguirre-Cabrera: Investigation, Review the draft. V. Carranza: investigation, writing review & editing. C. M. González Álvarez: formal analysis, investigation, writing original draft.

